High-resolution high-speed synchronous epifluorescence imaging of cardiac activation

Shien-Fong Lin,[a] Rashida A. Abbas, and John P. Wikswo, Jr.
Living State Physics Group, Department of Physics and Astronomy, Vanderbilt University, Nashville, Tennessee 37235

(Received 3 June 1996; accepted for publication 21 October 1996)

An optical imaging technique with high spatial and temporal resolution was developed to record fractional changes in laser-induced epifluorescence associated with the cardiac transmembrane potential during and after the application of monophasic point stimuli. The technique takes advantage of the repeatability of the recorded events, and uses a synchronized laser strobing mechanism to overcome the speed limitation inherent to slow-scan charge-coupled device cameras, and achieves an effective frame rate of 500 frames/s at a spatial resolution of 100×100 pixels in a single frame with a pixel resolution of 75 μm. The signal-to-noise ratio can be improved with boxcar averaging. Patterns of virtual cathode and anode with distinctive regions of simultaneous depolarization and hyperpolarization during stimulation are demonstrated with stimuli applied to the resting myocardium of an isolated rabbit heart. The technique described in this article provides a powerful tool for investigating repeatable dynamics in the function of electrically active tissue. [S0034-6748(97)03401-1]

I. INTRODUCTION

Cardiac activation is an important biophysical process directly relevant to the application of clinical arrhythmia treatment devices such as pacemakers and defibrillators. Traditionally, this phenomenon was studied using electrical recording approaches. In the last decade, cardiac optical mapping became an emerging technique which has been applied to preparations including cardiac cells,[1] two-dimensional slices of cardiac muscle,[2] and whole hearts.[3,4] Developed around the principle of staining the tissue with voltage-sensitive dyes and recording the variation in the intensity of the induced epifluorescence, a variety of approaches based on different light-sensing components have been utilized to measure the transmembrane potential (V_m) distribution during different electrical states in cardiac tissue. In principle, the V_m of a site on the tissue is estimated with $-\Delta F/F$, in which F is the fluorescence intensity obtained from the resting tissue, ΔF the variation of fluorescence intensity when the recording site of tissue is excited. The minus sign represents a decrease in F with a more positive V_m. The spatial variation in $-\Delta F/F$ can be recorded with sufficient accuracy to allow quantitative comparisons of theory and experiment that provide confirmation of the bidomain model for cardiac electrical behavior.

A major engineering compromise that has to be made during the system design is the trade-off between the spatial and temporal resolution of the recording. For example, photodiode arrays and laser scanning systems provide good time resolution at a limited number of points.[5–8] Fiber optic systems provide excellent signal-to-noise (S/N) ratios at one to four points, and can be used to map out cardiac activation patterns at a small number of locations by changing the recording sites of the ''optrode.''[9–11] Video techniques provide qualitative images with a large number of pixels and can be used to create movies of propagating activation and reentry.[2,12,13] However, the fixed acquisition rate of 60 frames/s and a 16.7 ms elapsed time between consecutive frames prohibits detailed observation of cardiac dynamics. Furthermore, digital video cameras typically have only a narrow dynamic range of 8-bit, or 256-level digitization, which creates a major drawback for quantitative studies of the transmembrane potential distribution. Because the change in fluorescence that corresponds to the transmembrane action potential is typically 5% of the background illuminance, an 8-bit dynamic range would generate data with only 12 digitized levels, i.e., 5% of 256, for signals of more than 100 mV in amplitude.

The system described in this article uses a high-sensitivity cooled charge-coupled device (CCD) camera as the optical detector. The sensitivity allows a short exposure duration that avoids the problems of dynamic image blurring and dye-bleaching. The 12-bit dynamic range of the camera and the frame-grabber provides a digitization of the transmembrane action potential of more than 150 levels. Most importantly, a synchronous-capture scheme, which locks the laser exposure timing to that of the stimulation, was devised to achieve an effective 500 Hz frame rate. All these engineering improvements in optical mapping techniques led to the successful observation of virtual electrode effects in cardiac activation.[4]

II. EXPERIMENTAL SETUP

The experiments were performed on the left ventricle of Langendorff-perfused isolated rabbit hearts. The voltage-sensitive dye di-4-ANEPPS (Molecular Probes, Eugene, Oregon) was added to the Tyrode's solution that perfused the heart at a concentration of 0.5 μM. The mechanical decou-

[a]Corresponding author; present address: Department of Physics & Astronomy, P.O. Box 1807, Station B, Nashville, TN 37235; Tel: (615) 343-0649; FAX: (615) 322-4977; Electronic mail: linsf@ctrvax.vanderbilt.edu

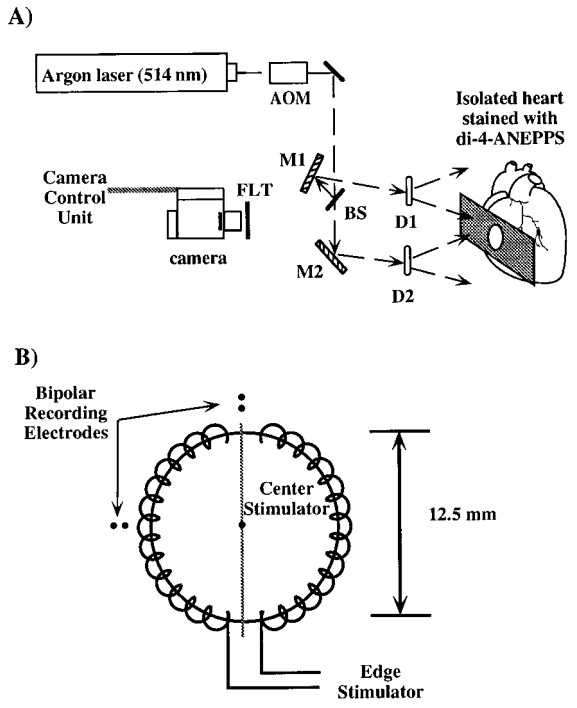

FIG. 1. (A) Schematic drawing of imaging setup. (B) The imaging window.

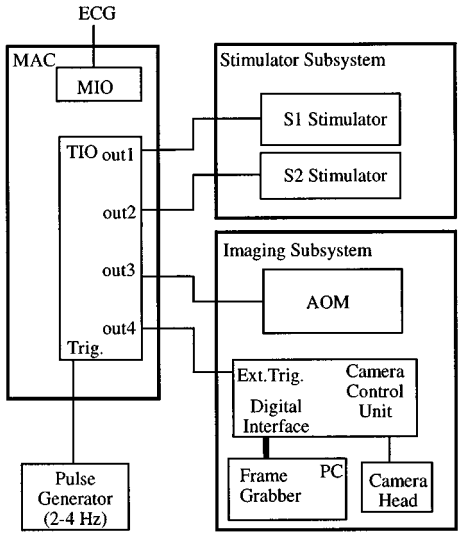

FIG. 2. Block diagram of the synchronous imaging system.

pler diacetylmonoxime (DAM, Sigma, St. Louis, MO) of 15 mM was added to the Tyrode's solution to inhibit muscle contraction.

The imaging system [Fig. 1(A)] consisted of a high-sensitivity digital cooled-CCD camera with 12-bit image digitization (Model 4100, Astrocam, Cambridge, England) with a 50 mm fl.8 objective lens (Pentax), and a 5 W argon laser (Innova 70-5, Coherent, Palo Alto, CA) with a 514 nm single line output of 1.5 W. An acousto-optical modulator (AOM, NEOS N23080, Melbourne, FL) served as a light-strobe mechanism for illuminating the heart. The internal mechanical shutter of the camera has an inherent induction delay of 11 ms, hence the minimum CCD exposure time is around 23 ms, far too long for observing dynamic cardiac events with millisecond rise time. The laser strobe light provided by the instantaneous beam deflection capability of the AOM, when working in the dark, serves as an effective fast shutter for imaging of dynamic events without significant blurring. The laser beam after the AOM was split in two with a 50/50 beam splitter (BS), each beam directed with mirrors (M1, M2) through ground glass diffusers (D1, D2) toward the imaging area on the heart. These two diffused beams were adjusted in position and distance to induce an approximately even and shadowless fluorescence from the imaging area.

The laser-induced fluorescence was filtered with a 570 nm long-pass colored glass filter (FLT) to remove the 514 nm inducing light before the camera. 100×100 pixel images covering a 7.5 mm$\times$7.5 mm field of view were taken through a circular 12 mm window opening in the planar electrode support that held stimulating and recording electrodes adjacent to the heart. In practice, an area of interest of 300×300 pixels out of a total of 768×520 pixels on the CCD was selected. A 3×3 binning operation on these selected pixels was performed to group adjacent nine pixels into a ''superpixel.'' The resulting image format thus became 100×100 superpixels. The binning is important to enhance the S/N ratio and lower the required laser intensity that would allow use of the full dynamic range of the CCD. During imaging, the isolated heart was pushed gently against the front circular window from the back side with a plastic supporting plate. A 1-cm-diam spiral of silver wire situated at the center of the supporting plastic plate on the opposite side of the heart was used as the reference electrode for electrical stimulation. Figure 1(B) shows a detailed schematic drawing of the imaging window. The short test stimuli were delivered through the center stimulator, which was a Teflon-insulated, 100 μm platinum wire wound two and half turns around a supporting suture stretched across the window. The Teflon insulation was removed from a central kink in the wire to allow the platinum to contact the epicardium over an area of 100 μm$\times$200 μm. A pair of platinum wires mounted along the edge of the window were used for additional conditional stimulation, providing the capability to ''prime'' the tissue to a predetermined electrical status such as depolarization or repolarization during the point stimulation. The timing and strength of both test and conditional stimuli provided the necessary combination of stimulation for different experiments.

The block diagram shown in Fig. 2 illustrates the control and wiring of the system. The electrocardiogram (ECG) signals obtained from the bipolar electrodes attached to the imaging window were continuously monitored through a multiple input/output (MIO) card installed in a computer. The synchronous-imaging setup, which locked the laser exposure to that of the onset of electrical stimulation, was devised to achieve an equivalent 500 Hz frame rate, taking advantage of the repeatability of cardiac activation events. The core of the system was a programmable timing device (TIO) producing timing signal with variable delay and duration. TIO was triggered by the periodic pulses from the pulse generator, and generated four timing signals for stimulating the tissue (S1,

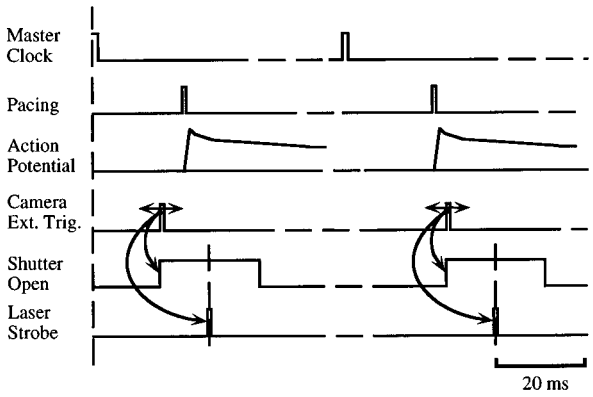

FIG. 3. Timing diagram of the system. Note that the ''shutter open'' and ''laser strobe'' signals are locked to ''camera external trigger'' with fixed delays.

S2), for strobing the light with AOM and for triggering the camera. The operation of the camera was controlled by the Camera Control Unit (CCU), which controlled the temperature of the camera, digitized the images, and fed the digital signal to the frame grabber in a personal computer.

Before the imaging, the sinus rhythm of the heart was captured by stimulator S1 at a rate slightly higher than the natural rhythm. During imaging, an image was taken for every trigger to the CCU. Therefore, the actual rate of imaging was the same as the frequency of the pulse generator (2–4 Hz). However, the progressive shift in the timing of the strobe light relative to the pacing stimulus could produce frame sequences with an effective frame rate much faster than the actual rate of imaging. In a typical imaging protocol, a sequence of 6–9 frames were taken with a successive 2 ms shift of timing in exposure, thus achieving an effective frame rate of 500 Hz.

Figure 3 shows the timing diagram of the system. For the monophasic current activation experiment, the S1 pacing pulse was locked to the master clock signal from the pulse generator with a constant delay of 20 ms. The pacing current pulse induced a propagating action potential beneath the center electrode. The camera trigger pulse activated the shutter, which became fully opened after 11 ms. The strobe light was delivered after this period of induction delay. It should be noted that because all the timing signals were synchronized to the master clock, box-car averaging technique can be employed to enhance the S/N ratio by repeating the timing sequence of imaging.

III. RESULTS AND DISCUSSION

In cardiac electrophysiology, the virtual electrodes are the regions of tissue that are instantaneously depolarized (virtual cathodes) or instantaneously hyperpolarized (virtual anode) by the stimulus pulse.[14] For strong stimuli that are 10 to 20 times threshold, the virtual electrodes can have a spatial extent several orders of magnitude larger than the actual stimulus electrode. The relationship between virtual electrodes and tissue anisotropy is reviewed in detail elsewhere.[15,16] The objective of the present study was to obtain high spatial and temporal resolution images of the transmembrane potential distribution adjacent to the virtual electrodes during several different modes of stimulation.[4] Because the information describing the transmembrane potential distribution is embedded in the modulation of the background fluorescence level, image processing is required to extract such information from the raw images and to enhance the S/N ratio.

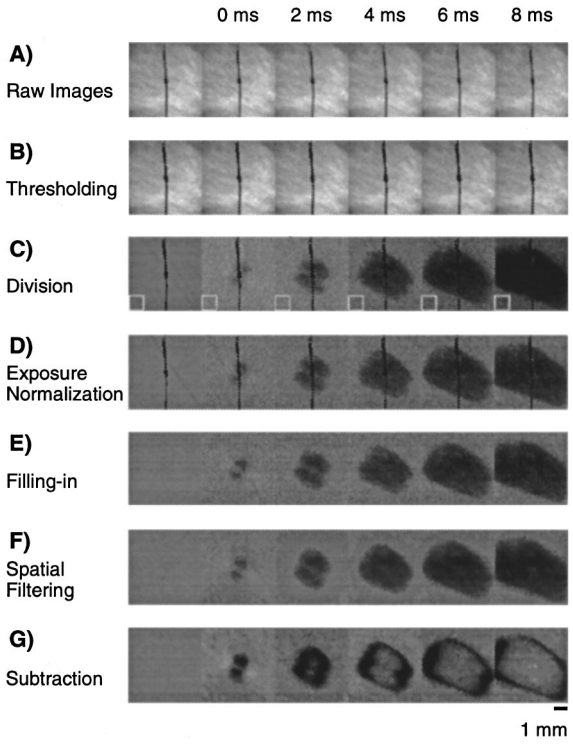

FIG. 4. The sequence of image processing on a frame sequence of cardiac activation following monophasic, cathodal stimulation. The muscle fiber axis runs from lower right to upper left. In all the sequences except A and B, black is depolarization and white is hyperpolarization.

Figure 4 shows the results from each step in the image processing procedure. The sequence in Fig. 4(A) shows the raw epifluorescence images. The region covered by the suture supporting the stimulation electrode, which appeared as a black line in the images, can be detected by a threshold process to identify the pixels with low intensity [Fig. 4(B)]. These low-intensity pixels were inhibited from further mathematical operations because they carried no significant information. The transmembrane potential distribution [Fig. 4(C)] was obtained by dividing the image to be processed with the image obtained immediately before the delivery of the electrical stimulus [the left-most frame in Fig. 4(B)], when all of the tissue in the imaging area was at its resting, diastolic potential.

The background levels of each of the frame in Fig. 4(C) are not equal due to the temporal instability of the laser output energy, as evidenced by different gray levels in the as-yet depolarized region in each frame. Such a variation was accounted for by a normalization procedure, which selected a region of tissue that remained at rest throughout the sequence [the regions in the white squares in Fig. 4(C)], and normalized each frame to the average intensity of that region. To further enhance the S/N ratio, digital filtering can be em-

ployed to remove the appearance of pixels for easier visualization of regions with meaningfully different fluorescence levels. However, the spatial filtering operation would smear the region of the suture into the neighboring region. We filled the suture region with random numbers that had a mean and variance calculated from the adjacent pixels. In our application, at each point along the suture, we used the mean and the variance of the three pixels on both sides of the suture. The results after random filling and the subsequent spatial filtering are shown in Figs. 4(E) and 4(F). To facilitate the observation of the propagating wave fronts, a ''difference'' image sequence [Fig. 4(G)] was generated by subtracting successive frames, which produced the propagating wave fronts similar to a derivative operation in the time domain. The gray-scale in Fig. 4(G) was adjusted to accommodate the smaller signal level and to facilitate visualization. The dog-bone virtual cathode and the adjacent regions of virtual anode became apparent as predicted by theory. The gray-scale can be converted to pseudo-color for illustration purposes.

In contracting hearts, the optical properties of tissue change dynamically with the inhomogeneous heart wall movement. Such changes would significantly alter the detected fluorescence due to the time-varying optical absorption-excitation relationship in dye-stained tissue. In order to avoid such spurious changes in the background fluorescence, cardiac optical recording procedures are usually performed with the muscle movement blocked by introducing mechanical decoupling agents such as DAM, which was found to have minimal effects on cardiac cell membrane conductances.[17,18] The resulting stable background fluorescence intensity in the resting tissue is necessary for the execution of the normalization procedure described in this article. An additional requirement for a satisfactory normalization is some *a priori* knowledge of the tissue status in each frame to be normalized. This is straightforward in activation studies, because the wave front propagates outwardly from the point stimulus in a regular way. However, this situation does not apply to irregular wave front propagation such as during fibrillation.

In this study, the synchronous imaging system was used to record cardiac activation with a small point electrode delivering monophasic stimuli. Although previous theoretical calculations have shown the existence of complex patterns associated with such stimulation procedures, detailed visualization of such patterns has not been possible until the application of the current system.[4] Such a technique using slow-scan digital cameras is suitable for observing repeatable dynamic events, such as cardiac activation under a periodic captured rhythm. Similar techniques can also be applied using a video camera for observing repetitive events, however, with mostly an 8-bit dynamic range.[19] Lower sensitivity and limited synchronization capability inherent to most video cameras make them useful only for imaging propagation of cardiac wave fronts. On the other hand, cooled-CCD cameras have low dark current of approximately 5 electron/pixel/second at $-40\,^{\circ}\mathrm{C}$, which is negligible for short exposure duration of only a few milliseconds, and thus can provide high sensitivity for low-level fluorescence. Cooled-CCD cameras, combined with the additional capability of synchronous laser strobing, are at present the device of choice for studies of the transmembrane potential distributions during and after direct activation.

Our approach represents a compromise that provides high spatial resolution, 0.5 ms exposure times, a 2 ms or shorter frame interval, and a 12-bit dynamic range. It is possible to further reduce the exposure duration with the synchronous imaging technique, and therefore to further reduce the blurring of wave front edges due to propagation. However, because the AOM has a fixed contrast ratio of 500:1, a short exposure will result in a reduced signal amplitude and fewer gray scales in the images. Imaging of cardiac action potentials should not require exposures of less than several hundred microseconds, as demonstrated by a fiber optic system.[9–11] However, such short exposures for a large-area imaging system will require either higher laser power, with the concomitant risk of dye bleaching, or the use of one- or two-stage image intensifiers, which may compromise the spatial resolution. On the other hand, shortening the frame interval could lead to a large increase in the number of frames in a movie, presenting problems of data transfer and storage.

The synchronous technique is at present limited to using box-car averaging techniques to create movies that are only several frames long. The studies of asynchronous or nonstationary phenomena such as ectopic beats, reentry, or fibrillation are not possible with the system. Future enhancements to our camera should extend the capabilities of the imaging system to imaging asynchronous events. Some realistic improvements would include removing the slow mechanical shutter and replacing the current image sensor to a frame-transfer CCD, as well as employing a laser stabilizer to reduce the instability in laser output power. With the rapid progress in the resolution and speed of commercial large-format CCD cameras, it can be expected that direct imaging of aperiodic cardiac events should be possible in the near future.

ACKNOWLEDGMENTS

This study was supported by NIH Grant No. P01HL46681, and by an NIH training grant 5T32 HL07411-16A1 and a Biomedical Engineering Research grant from the Whitaker Foundation to S. F. L.

[1] V. G. Fast and A. G. Kléber, Circ. Res. **73**, 914 (1993).
[2] J. M. Davidenko, A. M. Pertsov, R. Salomonsz, W. T. Baxter, and J. Jalife, Nature (London) **355**, 349 (1991).
[3] S. B. Knisley, T. F. Blitchington, B. C. Hill, A. O. Grant, W. M. Smith, T. C. Pilkington, and R. E. Ideker, Circ. Res. **72**, 255 (1993).
[4] J. P. Wikswo, Jr., S.-F. Lin, and R. A. Abbas, Biophys. J. **69**, 2195 (1995).
[5] S. B. Knisley and B. C. Hill, Circulation **88**, 2402 (1993).
[6] G. Salama, A. Kanai, and I. R. Efimov, Circ. Res. **74**, 604 (1994).
[7] M. G. Fishler, R. Ranjan, and N. V. Thakor, Proceedings of the 16th Annual International Conference of the IEEE Engineering in Medicine and Biology Society, 1994, Vol. 16, pp. 9–10.
[8] B. C. Hill and K. R. Courtney, Ann. Biomed. Eng. **15**, 567 (1987).
[9] S. M. Dillon, Circ. Res. **69**, 842 (1991).
[10] M. Neunlist, S. Z. Zou, and L. Tung, Pflügers Arch. **420**, 611 (1992).
[11] M. Matual, S. F. Lin, M. Brooks, Y. Shyr, R. Province, B. Pless, and D. S. Echt, PACE **19**, 623 (1996).
[12] G. Nassif, S. Dillon, and A. L. Wit, J. Mol. Cell. Cardiol. **22** (Suppl. IV), S.44 (1990).

[13] A M. Pertsov, J. M. Davidenko, R. Salomonsz, W. T. Baxter, and J. Jalife, Circ. Res. **72**, 631 (1993).
[14] J. P. Wikswo, Jr., T. A Wisialowski, W. A. Altemeier, J. R. Balster, H. A. Kopelman, and D. M. Roden, Circ. Res. **68**, 513 (1991).
[15] J. P. Wikswo, Jr., in *Cardiac Electrophysiology: From Cell to Bedside*, edited by D. P. Zipes and J. Jalife (Saunders, Orlando, FL, 1994), pp. 348–361.
[16] B. J. Roth and J. P. Wikswo, Jr., Proc. IEEE **84**, 379 (1996).
[17] T. Li, N. Sperelakis, R. E. Teneick, and R. J. Solaro, J. Pharmocol. Exp. Ther. **232**, 688 (1984).
[18] Y. Liu, C. Cabo, R. Salomonsz, M. Delmar, J. Davidenko, and J. Jalife, Cardiovasc. Res. **27**, 1991 (1993).
[19] M. Möller and H.-J. Bruns, Rev. Sci. Instrum. **66**, 4535 (1995).